

Design and Implementation of Z Source Resonant Converter for EV Wireless Charging Application

Athira Rajan¹, Saneep K², Sreenath K M³, Prasanth R K⁴

¹PG Student, ²PG Student, ³PG Student, ⁴Asst. Professor,

EEE Dept., NSS College of Engineering, Palakkad, Kerala, India

Abstract - Wireless Power Transfer (WPT) technology is an emerging research area due to its safety and convenience. A Conventional WPT system has Front End PFC and DC-DC Boost Converter, which makes the system bulkier. The Z Source Inverter (ZSI) was introduced into WPT systems to improve the system performance. The ZSI regulates the input voltage in WPT systems without Front End Converters and makes the inverter bridge immune to Shoot Through (ST) states. This paper includes the design and implementation of an inductive power transfer system for wireless charging of future electric transportation using Z Source Resonant Converter. In addition, fabrication and control of an efficient series-series resonant inductive power transfer (SS-RIPT) system for electric vehicle battery charging application. The results are through simulations and finally, the designed system is implemented experimentally.

Keywords - Wireless, Power Transmission, Electric Vehicle, Charging

I. INTRODUCTION

Wireless Power Transfer (WPT) systems are designed to transfer power efficiently from a stationary primary coil to a stationary or movable secondary coil through an air gap. Contactless means inductive coupling between two objects through an air gap. The fundamental principle of a WPT system is similar to the closely coupled electrical and electromechanical devices such as transformers and induction motors in which leakage inductance is very low due to high magnetic coupling. But WPT systems are operated at a large air gap resulting in high leakage inductances and low magnetic coupling. Due to high leakages and low magnetic coupling, WPT systems have very poor power transfer efficiency. In order to offset the effect of low magnetic coupling due to high magnetic leakages, WPT systems are generally operated at high frequencies to improve the quality factor of the WPT transformer. On the other hand, at high frequencies, losses in the system will be increased due to high switching losses of the inverter and thereby affecting the overall power transfer efficiency of the system. To overcome this drawback, WPT systems are commonly operated at resonant frequency by incorporating compensating capacitors. Presently, the operational frequency for high

power WPT systems is below 100 kHz due to high switching losses at a high frequency. Additionally, resonant circuits reduce the reactive power requirement for the system thereby boosting the overall power transfer capability and minimizing the VA (Volt-Ampere) ratings of the system.

WPT technology deliver power through an electromagnetic field without any physical connection between the transmitter and receiver [1]-[3]. Recent advancements in this field have led to more stringent design requirements being proposed and studied by researchers, such as efficiency improvement [4]-[8], coupling variation [9], [10], foreign object detection [11], [12], and output regulation [13]-[15]. Electronic technology plays a crucial role in these research studies and spurs WPT technology development. The voltage source inverter (VSI) is an essential part of a WPT system that generates high-frequency ac power for transmission across a wireless media. Unfortunately, the output voltage of conventional VSI is always is equal to or lower than the input voltage, which limits this inverter's application in small-voltage or wide input situations. To address this barrier, front-end converters, such as boost converter or buck-boost converter are inserted between a dc source and a VSI to boost the dc-rail voltage [16], [17]. However, this require more space and increase the cost of the system. To add one additional IGBT/MOSFET one extra heat sink and associated drive circuitry is to be accommodated. Considering the incremental cost and design complications, the ZSI presents a better alternative to front-end converters in WPT system.

When compared with a conventional VSI, the ZSI has an input diode DS and a Z-source network added between the dc voltage source and the VSI [18]. The Z-source network consists of two identical inductors (L1 and L2) and capacitors (C1 and C2) to boost the output voltage by shorting one or two legs of the rear-end inverter bridge. This is also referred to as the shoot-through (ST) state.

Guidelines to design Z-source network based on steady state parameters were presented in [19]. Since the network

is connected to a three-phase VSI, the output current of the network is regarded as a constant current. Meanwhile, the current in the network of WPT system is approximately sinusoidal over part of one switching period due to a sinusoidal resonant current. The mathematical analysis in [19] is modified when applied to a WPT system. In [20], the benefits of a ZSI in resonant converters are analyzed. These benefits include improved robustness and reliability, buck/boost function, and high efficiency over wide input and load ranges.

The ZSN in the proposed ZSRI provides the unique feature of inherent power factor correction (PFC) without adding extra switching devices. It is possible because it adds the unique features of immunity to the H-bridge inverter during shoot-through states. This characteristic makes the input current as a sinusoidal waveform and in phase with the ac input voltage. This variable also provides a boost factor to the system. However, to regulate the output voltage, the proposed ZSN-based inverter uses the active state duty cycle, which is a common control variable used in series resonant inverters. Both control variables are used in the series resonant H-bridge inverter and the ZSRI does not require additional control circuitry to provide power factor correction. In other words, because of the ZSN, the ZSRI can perform power factor correction as well as dc/ac conversion in single stage.

II. WIRELESS CHARGING SYSTEM FOR EVS

The transport sector alone accounts for approximately 23% of the total energy-related emissions [13]. EVs are seen as a viable solution to the growing pollution problem. However, the major hurdle in the broad acceptance of EVs is attributed to their high battery cost and limited driving range.

The Li-Ion battery is widely used as the primary power source for the EV's drivetrain due to their high specific energy (100-265 Wh/kg) and specific power density (250-340 W/kg) compared to other battery technology. Despite its superior characteristics, it still adds considerable weight and size to the vehicle. For example, Nissan Leaf's 24 kWh battery pack weighs around 200 kg. In addition to high weight and size, the estimated cost of the battery pack is about US\$700/kWh. Therefore, the price of an EV is almost double that of a gasoline counterpart with nearly half of the cost for the battery itself [14].

The limited driving range is an even greater obstacle to the market penetration of EVs than their higher cost. For example, gasoline vehicles can go over 500 km before refuelling which takes about 2-3 minutes at a filling station which are located every few kilometers. On the other hand, most EVs can only go about 100-200 km before recharging, and take a long charging time [15]. For example, Level 2 charging circuit of 9.6 kW power takes

about 1.5 hrs, to fully charge the battery pack of the Chevrolet Volt [16]. Besides this, charging stations are not as readily available as fuel stations. These limitations of EVs have been termed as 'range anxiety' issue for obvious reasons.

The aforementioned limitations of EVs can be overcome by adopting wireless charging technology for EV battery charging which provides the following advantages over conventional wired charging: reasons.

Range Extension: Wireless charging has the scope for 'opportunity charging' i.e. charging the vehicle little and often during the day when the EV is not in use [17]. For example, in addition for residential garage, public and private parking areas, the wireless charger can also be installed at: traffic lights; bus stops; high traffic congestion area where vehicles are slow moving; and taxis ranks that move forward as taxis are hired [18]. These opportunity charging are possible since wireless charging does not require human intervention and therefore charging can be carried out automatically. This in turn leads to significant improvements in range compared to that available from a single overnight plug-in charge.

Safety and Convenience: Wireless charging provides galvanic isolation between load and source. Therefore it eliminates the disadvantages of plug-in charging technology such as: risk of electrocution, especially in wet and hostile environment from aging wiring and bad connections; failure to plug in; trip hazard from a long connecting wire; poor visual appeal due to hanging cords; contactor wear caused by excessive use and thermal cycling; and, most importantly, discomfort in handling a plug-in charger in a harsh climate that commonly has snow and where the charge point may become frozen onto the vehicle [14], [19], [20].

Battery Volume Reduction: Due to the scope of opportunity charging, charging can take place more frequently. Therefore, EVs can travel the same distance with a reduced battery pack [13], [20]. This, in turn, can lower the price of EVs and make them more efficient due to the reduced weight. Frequent charging also extends the battery life by reducing the depth of discharge in the battery.

Weather Proof: In a wireless charger, power transfer takes place due to an electromagnetic link, therefore charging is not affected by the presence of snow, rain, or dust storms. Besides, a transmitter is embedded underground, therefore, is safe from extreme weather condition and requires less frequent maintenance or replacement than a plug-in charger would require.

In 2010 the Society of Automotive Engineers (SAE) assembled an international committee, known as SAEJ2954, to develop a working industry standard that

establishes the interoperability, frequency band, electromagnetic compatibility, minimum performance, safety, testing criteria as well as coils definitions for wireless charging of light duty electric and plug-in electric vehicles. The international committee includes automotive equipment manufacturers (OEMs), such as GM, BMW, Ford, Nissan and Toyota; Tier 1 suppliers Delphi, Panasonic and Magna; WPT suppliers, such as Qualcomm and LG, and a collection of other organizations, such as the Argonne National Laboratory, the EPA, the DOT, UL and the University of Tennessee.

Table-1: SAE J2954 Light Duty Vehicle WPT charging classes

| Classification | WPT1 | WPT2 | WPT3 | WPT4 |
|----------------|------------------------|------------------------|------------------------------|------------------------------|
| Power Levels | 3.7 kW | 7.7 kW | 11 kW | 22 kW |
| Status | Specified in TIR J2954 | Specified in TIR J2954 | To be Specified in TIR J2954 | To be Specified in TIR J2954 |

The current version of SAEJ2954 technical information report (TIR) was made available for purchase from the SAE website on May 31, 2016. The latest version addresses unidirectional charging from grid to vehicle and is intended to be used for static charging applications. Dynamic charging (charging while the vehicle is in-motion) and bidirectional power may be considered in the future based on industry feedback. This TIR specifies a common frequency band using 85 kHz band (81.39 kHz–90 kHz) for all light duty vehicle systems. In addition, it defines the power levels in four classes as shown in Table 1 .

III. Z SOURCE RESONANT CONVERTER

The ZSRC has more states in one switching cycle compared with other DC- AC systems. It is important to clarify all these states to understand the ZSRC. The boost ratio of ZSN is still related to the total shoot-through state duty cycle among these states. The operation principle of the ZSRC is described based here with an example of the phase-shift control method. Assuming that the ZSN is symmetrical ($C1 = C2 = C$, and $L1 = L2 = L$) therefore, $VC1 = VC2 = VC$, and $VC1 = VC2 = VC$. Also, the resonant frequency of L and C in ZSN is at least ten times smaller than the switching frequency. Hence, the ZSN inductor current and the ZSN capacitor voltage are considered to be constant in one switching cycle. Fig. 2 shows the conducting devices in different states—active state, shoot through state, and zero state.

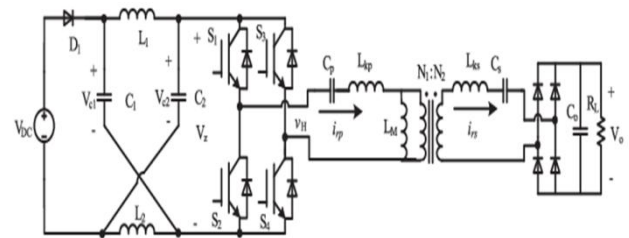


Fig.1. Circuit of WPT System with a ZSI

Active State: During the two active states time interval [see Fig. 6(c) and (g)], the diagonal switches are on, and the input side diode D1 is conducting. The resonant network draws current from both the ZSN inductor and capacitor. The difference between load current and ZSN inductor current is provided by a series connection of the two ZSN capacitor and dc source.

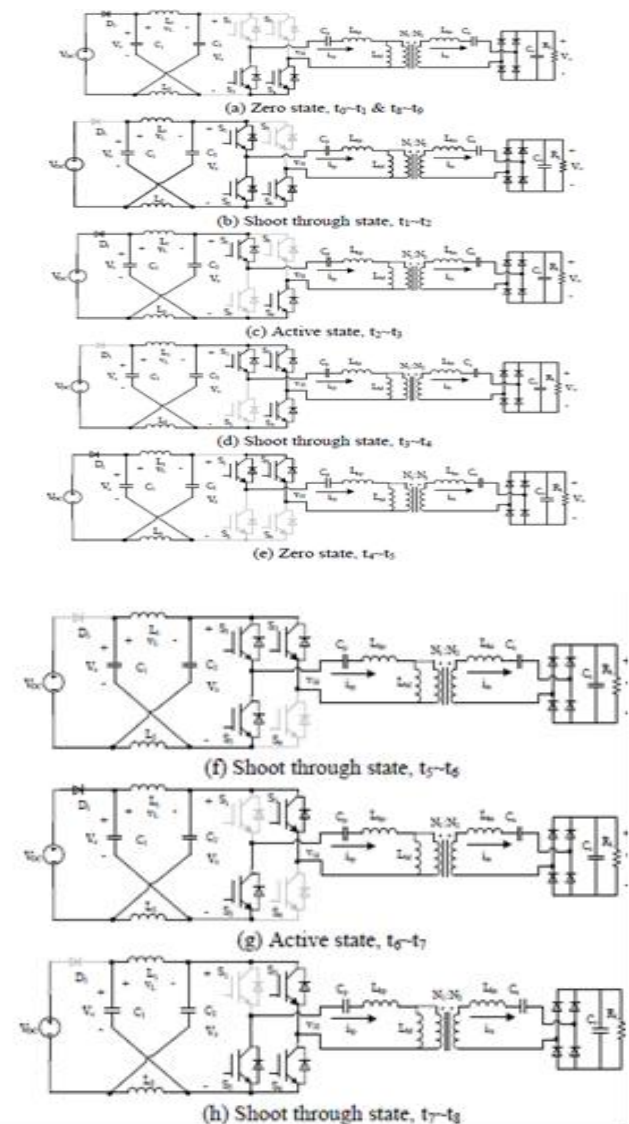


Fig.2. ZSRC circuit diagram in different states

The current going through the switches are only load current The ZSN inductor voltage for this time interval is given as,

$$V_L = V_{DC} - V_C \quad \dots(1)$$

Shoot-Through State: Three of the switches are ON. The two horizontal switches are carrying the load current and the switches in one-phase leg are carrying the ZSN inductor current. Hence, there is one switch carrying the sum of the two currents. Since the flow of ZSN inductor current is always in one direction and the load current would be bipolar, these two currents either subtract from each other or add together, contributing to the sum with their absolute value. Fortunately, phase-shift control only allows different polarity currents going through the same switch in shoot-through state. Here, the ZSN capacitors will charge ZSN inductors (this is how the ZSRC can boost the voltage). The ZSN inductor voltage for this time interval is given as,

$$V_L = V_C \quad \dots(2)$$

Zero State: During the zero state's time interval, two horizontal switches are ON. The ZSN is isolated from the load. The load current is freewheeling and the ZSN inductors charge the ZSN capacitors. The ZSN inductors voltage for this time interval is given as,

$$V_L = V_{DC} - V_C \quad \dots(3)$$

These three states are all the possible states in ZSRC. Different allocation of these three states along one switching period would generate different load regulation characteristic.

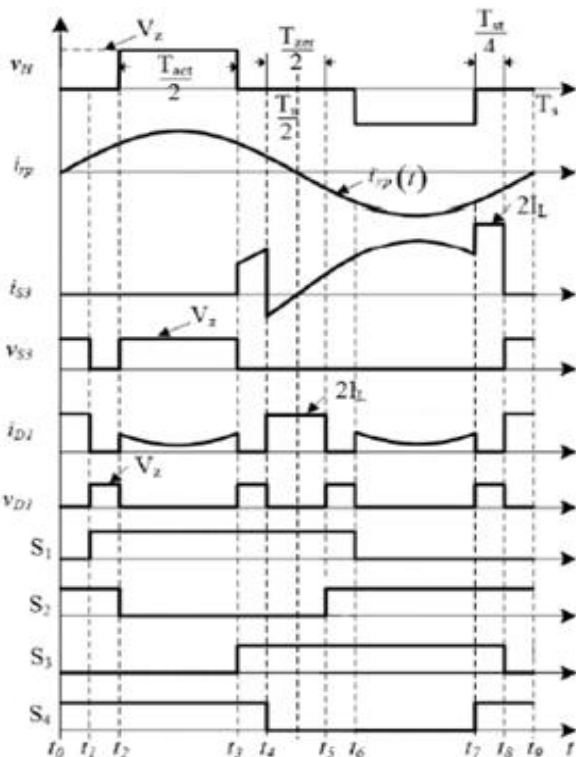


Fig.3. Time domain waveforms for phase shift control in ZSRC

IV. Z SOURCE RESONANT CONVERTER WPT SYSTEMS

The charging of plugin Electric Vehicles has always a safety risk of direct contact of metal to metal. To avoid this concern, the design of Electric Vehicle charging system were developed based on Inductive Power Transfer. The IPT works on Electromagnetic Induction phenomena to transfer power through the air cored transformer with closely spaced primary and secondary coils.

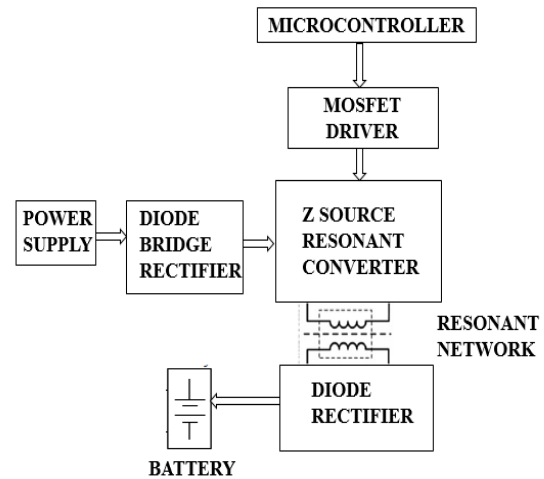


Fig.4. Block Diagram

The figure 4.1 gives the block of the Wireless power transfer for EV charging with high power transfer capability. There are mainly four blocks in the system, the power supply, Diode Bridge, converter block and the Wireless network. at first ac voltage V_{ac} (phase voltage) is rectified into DC voltage V_{dc} by a diode bridge rectifier. This DC link voltage serves as the DC input voltage to the Z-source network. The DC output voltage of the Z source network is converted into a high frequency single phase ac voltage by an MOSFETs-based full-bridge resonant inverter for WPT system.

The Microcontroller block that sends corresponding pulses that varies the output accordingly at the converter stage. The voltage pulses send by the microcontroller might not be large enough to drive the MOSFETs in the converter stage, so these pulses are fed to the MOSFET driver stage where the signals will be amplified enough to drive the MOSFET in the converter stage.

In the proposed system we use ATMEGA 328 as the microcontroller. Its operating voltage range is 2.5V-5.5V. The MOSFET used in converter section is the IRFP250N. In the MOSFET driver stage opto coupler is used. The opto coupler which is used here is TLP250H.

V. CIRCUIT DIAGRAM

According to the placement of the compensation capacitors on the primary and secondary sides, there are four basic

topologies: Series-Series (SS), Series-Parallel (SP), Parallel-Series (PS) and Parallel-Parallel (PP). The ZSI creates a new control state, called the ST state, where at least one leg of the inverter is shorted. Thus, the inverter is effectively short-circuited at that time. If the primary side adopts a parallel compensation capacitor (PS and PP), the resonance path breaks because the terminals of the transmission coil and compensation capacitor are shorted at the ST state, and the energy stored in the compensation capacitor is discharged through switches. Therefore, series compensation on the primary side (i.e., SS and SP) is recommended.

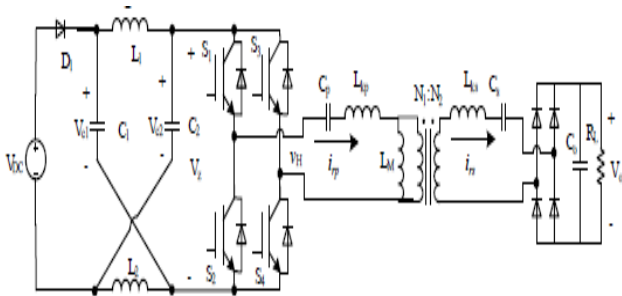


Fig.5. Circuit Schematic of the Z Source Resonant Converter.

VI. SIMULATION RESULTS

The input voltage of the ZSRC is $V_s=33V$ and the output voltage and current is $V_o=88v$ and $I_o=2.28A$ with the resonant frequency of $20kHz$. Assuming that the ZSN is symmetrical ($C1 = C2 = C$, and $L1 = L2 = L$) therefore, $V_{C1} = V_{C2} = V_C$, and $V_{L1} = V_{L2} = V_L$. Also, the resonant frequency of L and C in ZSN is at least ten times smaller than the switching frequency. Hence, the ZSN inductor current and the ZSN capacitor voltage are constant in one switching cycle.

The significant part of the design is choosing the inductor and capacitor values and operating frequency. On the contrary, use of the low frequency leads to increases both on the size and also the cost of inductors and capacitors. Thus, there is a trade-off between the size and efficiency in determining the operating frequency of the converter. The frequency is selected as $20kHz$.

Simulation has been performed and the results are presented for each converter stage. The circuit consists of a high frequency (HF) Z Source Resonant Converter. High frequency switching is implemented using MOSFET switches. This is the high frequency link. A HF transformer provides voltage transformation and isolation between the DC source and the load. At the output side, a full bridge rectifier is connected to load. For analytical study, a resistive load is selected. The closed loop is controlled for constant output.

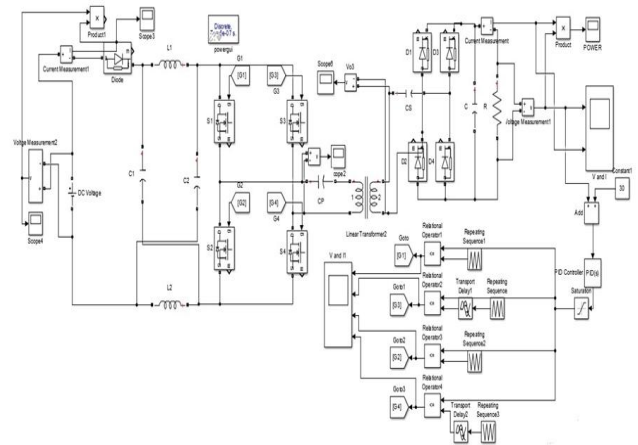


Fig.6. Simulation Diagram of ZSRC for WPT

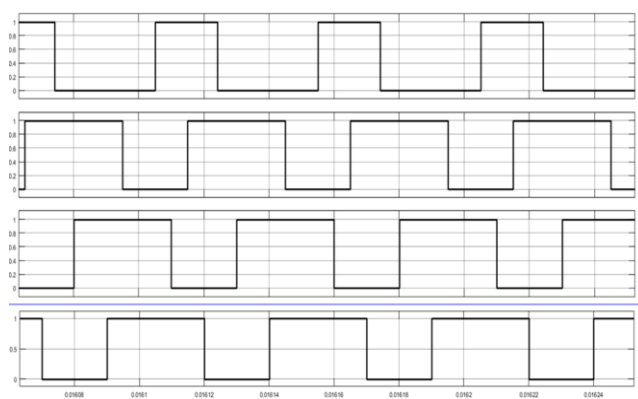


Fig.7. Waveform of gating signal for MOSFETS

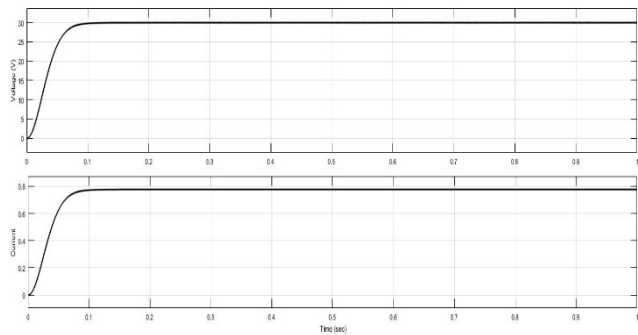


Fig.8. Waveform of output voltage and output current of the ZSRC

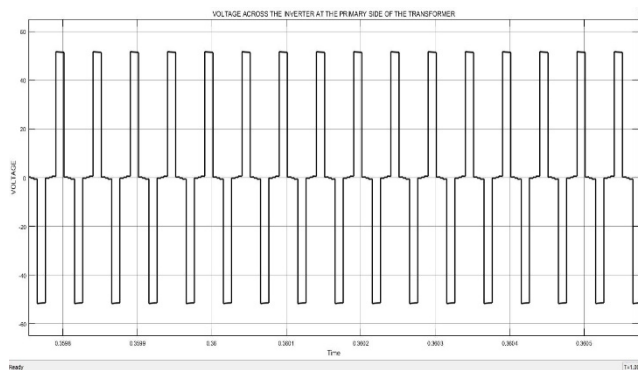


Fig.9. Voltage across the H Bridge at the primary side

VII. HARDWARE IMPLEMENTATION

The main circuit diagram consists of four sections, converter section, control section, driver section and power circuit. The converter section consists of four IRFP460N MOSFETs. Even if there is any fluctuations in the input the output will be maintained constant by the program stored in the microcontroller. Microcontroller sends the corresponding signals, which will be too feable to drive the MOSFET switches, so a driver circuit consisting of TLP250 Driver are used which boosts the amplitude of the signals enough to drive the switches.

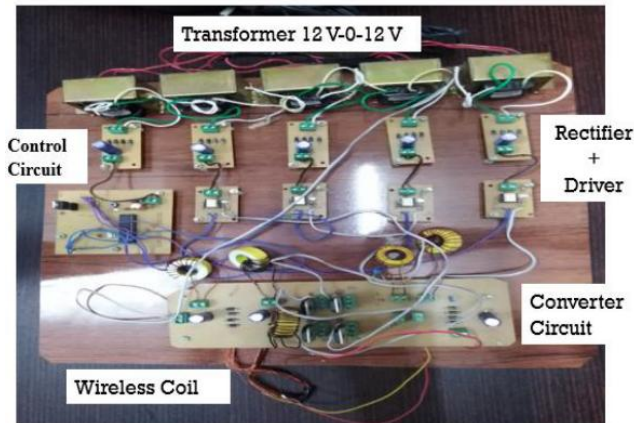


Fig.10. Complete Hardware Setup

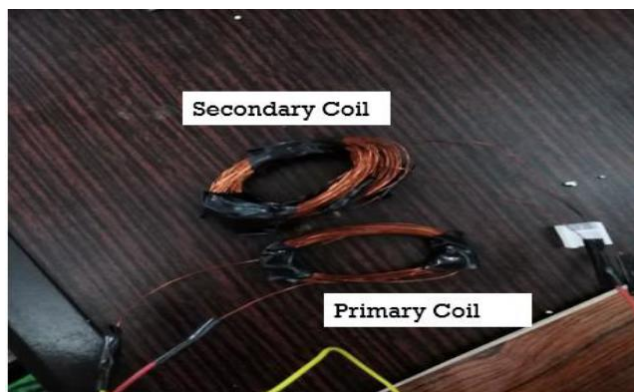


Fig.11. Wireless Power Transfer Setup



Fig.12. Output Obtained

VIII. CONCLUSION

A new circuit topology for high power WPT applications using a full bridge Z-source resonant inverter has been developed and simulated. The control methods in the

system with the insertion of shoot-through modes of the Z-source inverter have been investigated. In simulation, ideal MOSFETs and diodes were used. The output voltage of 27 V and output current of 0.9 A, i.e output of 23.5 W is obtained for the coupling coefficient k of 0.2. In the experiment, an output current of 0.9 A, and output voltage of 16 V was obtained. The slight difference between the simulation and experimental results is due to the following reasons: Core losses, simulation-ideal diode and MOSFET switches were used. Nevertheless, in both the simulation and experiment, the results obtained are very close to the analytical design value. This, in turn, validates the designed parameters.

REFERENCES

- [1]. Kurs, A. Karalis, R. Moffatt, J. D. Joannopoulos, P. Fisher, and M. Soljacic, "Wireless power transfer via strongly coupled magnetic resonances," *Science*, Vol. 317, pp. 83-86, Jul. 2007.
- [2]. J. T. Boys and G. A. Covic, "The Inductive Power Transfer Story at the University of Auckland," *IEEE Circuits Syst. Mag.*, Vol. 15, No.2, pp. 6-27, May 2015
- [3]. H. Vázquez-Leal, A. Gallardo-Del-Angel, and R. Castañeda-Sheissa, "The Phenomenon of Wireless Energy Transfer: Experiments and Philosophy," in *Wireless Power Transfer- Principles and Engineering Explorations*, InTech, Chap. 1, pp. 1-18, 2012.
- [4]. R. Melki and B. Moslem, "Optimizing the design parameters of a wireless power transfer system for maximizing power transfer efficiency: A simulation study," in *Technological Advances in Electrical, Electronics and Computer Engineering (TAECE)*, pp. 278-282, 2015
- [5]. Wang, H. Zhang, and Y. Liu, "Analysis on the efficiency of magnetic resonance coupling wireless charging for electric vehicles," in *Cyber Technology in Automation, Control and Intelligent Systems (CYBER)*, pp. 191-194, 2013.
- [6]. Kallel, O. Kanoun, T. Keutel, and C. Viehweger, "Improvement of the efficiency of MISO configuration in inductive power transmission in case of coils misalignment," in *Instrumentation and Measurement Technology Conference (I2MTC) Proceedings*, pp. 856-861, 2014.
- [7]. M. Fu, T. Zhang, C. Ma, and X. Zhang, "Efficiency and Optimal Loads Analysis for Multiple-Receiver Wireless Power Transfer Systems," *IEEE Trans. Microw. Theory Techn.*, Vol. 63, No. 3, pp. 801-812, Mar. 2015.
- [8]. Z. Low, R. Chinga, R. Tseng, and J. Lin, "Design and test of a high-power high-efficiency loosely coupled planar wireless power transfer system," *IEEE Trans. Ind. Electron.*, Vol. 56, No. 5, pp. 1801-1812, May 2009.
- [9]. O. Jonah, S. V. Georgakopoulos, D. Daerhan, and Y. Shun, "Misalignment-insensitive wireless power transfer via strongly coupled magnetic resonance principles," in *Antennas and Propagation Society International Symposium (APSURSI)*, pp. 1343-1344, 2014.

- [10]. H. Feng, T. Cai, S. Duan, J. Zhao, X. Zhang, and C. Chen, "An LCC-compensated resonant converter optimized for robust reaction to large coupling variation in dynamic wireless power transfer," *IEEE Trans. Ind. Electron.*, Vol. 63, No. 10, pp. 6591-6601, Oct. 2016.
- [11]. N. Kuyvenhoven, C. Dean, J. Melton, J. Schwannecke, and A. Umenei, "Development of a foreign object detection and analysis method for wireless power systems," in *Product Compliance Engineering (PSES) Proceedings*, pp. 1-6, 2011
- [12]. G. Jang, S. Jeong, H. Kwak, and C. Rim, "Metal object detection circuit with non-overlapped coils for wireless EV chargers," in *Southern Power Electronics Conference (SPEC)*, pp. 1-6, 2016.
- [13]. L. Tan, S. Pan, C. Xu, C. Yan, H. Liu, and X. Huang, "Study of constant current-constant voltage output wireless charging system based on compound topologies," *J. Power Electron.*, Vol. 17, No. 4, pp. 1109-1116, Jul. 2017.
- [14]. L. Sun, H. Tang, and C. Yao, "Investigating the frequency for load-independent output voltage in three-coil inductive power transfer system," *Int. J. Circ. Theor. Appl.*, Vol. 44, No. 6, pp. 1341-1348, Aug. 2015
- [15]. L. Zhang, X. Yang, W. Chen, and X. Yao, "An isolated soft-switching bidirectional buck-boost inverter for fuel cell applications," *J. Power Electron.*, Vol. 10, No. 3, pp. 235-244, May 2010.
- [16]. R. Mosobi, T. Chichi, and S. Gao, "Modeling and power quality analysis of integrated renewable energy system," in *National Power Systems Conference (NPSC)*, pp. 1-6, 2014
- [17]. F. Peng, "Z-source inverter," *IEEE Trans. Ind. Appl.*, Vol. 39, No. 2, pp. 504-510, Mar. 2003.
- [18]. S. Rajakaruna and L. Jayawickrama, "Steady-state analysis and designing impedance network of z-source inverters," *IEEE Trans. Ind. Electron.*, Vol. 57, No. 7, pp. 2483-2491, Jul. 2010.
- [19]. H. Cha, F. Peng, and D. Yoo, "Z-source resonant DC-DC converter for wide input voltage and load variation," in *Power Electronics Conference (IPEC)*, pp. 995-1000, 2010.
- [20]. H. Zeng and F. Z. Peng, "SiC based z-source resonant converter with constant frequency and load regulation for EV wireless charger," *IEEE Trans. Power Electron.*, Vol. 32, No. 11, pp. 8813-8822, Nov. 2017.
- [21]. T. Wang, X. Liu, H. Tang, and M. Ali, "Modification of the wireless power transfer system with Z-source inverter," *IET Electron. Letters*, Vol. 53, No. 2, pp. 106-108, Jan. 2017.
- interests are Power electronics, Special Electrical Machines, Renewable Energy Sources and AC Machines.
- Saneep K** has received his Bachelor of Technology degree in Electrical & Electronics Engineering from University of Calicut, in the year 2018. At present, he is pursuing M.Tech with the specialization of Power Electronics in NSS College of Engineering, Palakkad. His area of interests are Control System, Power electronics, Electric Drives, Hybrid Electric Vehicles and Power Converters.
- Sreenath K M** has received his Bachelor of Technology degree in Electrical & Electronics Engineering from University of Calicut, in the year 2016. At present, he is pursuing M.Tech with the specialization of Power Electronics in NSS College of Engineering, Palakkad. His area of interests are Power electronics, Signal and Systems, Power System.
- Prasanth R K** has received his Bachelor of Technology degree in Electrical & Electronics Engineering from Tamilnadu College of Engineering in the year 2013 and M.Tech with the specialization of Power Electronics and Drives from JCT College of Engineering and Technology. At present, he works as Assistant Professor in NSS College of Engineering, Palakkad. His area of interests are Power electronics and Wind Energy

AUTHOR'S PROFILE

Athira Rajan has received her Bachelor of Technology degree in Electrical & Electronics Engineering from University of Calicut, in the year 2017. And she completed her M.Tech with the specialization of Power Electronics from NSS College of Engineering, Palakkad. Her area of